Earth, Planets and Space

FULL PAPER Open Access

Crustal density structure investigation of the East China Sea and adjacent regions using wavenumber domain 3D density imaging method

Huiyou He[1,2], Heping Sun[1], Jian Fang[1*], Dongmei Guo[1] and Jinbo Li[1,3]

Abstract

The East China Sea, situated at the intersection of the Eurasian, Philippine Sea, and Pacific plates, is characterized by complex geology influenced by tectonic phenomena such as plate movements, volcanism, faults, and uplifts. Crustal density structure inversion provides a thorough understanding of the region's geological history as well as Earth's dynamical evolution, providing critical insights into seismic disaster mitigation, resource exploration, marine environmental protection, and maritime safety. The inversion process, on the other hand, presents challenges in data quality, quantity, model complexity, uncertainty, and computational resources. With the advancement of next-generation satellite gravity measurements and developing inversion techniques, the inversion of marine crustal density structures promises to be more precise and comprehensive. We explored the density distribution in the East China Sea and surrounding areas using an innovative wavenumber domain three-dimensional density imaging method along with high-precision global satellite gravity data. By overcoming data quality and computing resource constraints, wavenumber domain three-dimensional density imaging has transformed the discipline of marine geophysics, successfully delivering accurate density distributions in the study area. We were able to get a more precise and comprehensive characterization of the crustal density structure by combining high-precision satellite gravity data and cutting-edge imaging methods. Our investigation has unveiled previously unknown details about density distribution in the East China Sea and its environs. The East China Sea shelf displays smooth low-density perturbations at 18 km depth, whereas the trench–arc–basin region exhibits increasing density perturbations. Notably, the Okinawa Trough, which is surrounded by the Tokara Volcanic Ridge and the Ryukyu Trench, displays strong positive anomalies with a north–northeastern to northeastern orientation. In contrast, the Ryukyu Ridge and the Philippine Sea Basin exhibit smaller negative values and substantial northwestward positive density trends, respectively. These findings indicate diverse material distribution, which provides important insights into the area's geological evolution and tectonic processes. This study adds new insights into density distribution in the East China Sea and adjacent regions, offering information on the geological complexity of the region. The research lays the groundwork for future research on crustal dynamics and enhances the field of marine geophysics and related disciplines.

Keywords East China Sea, Crustal density, Wavenumber domain 3D density imaging, Satellite gravity data, Geodynamic evolution

*Correspondence:
Jian Fang
jfang@whigg.ac.cn
Full list of author information is available at the end of the article

Graphical abstract

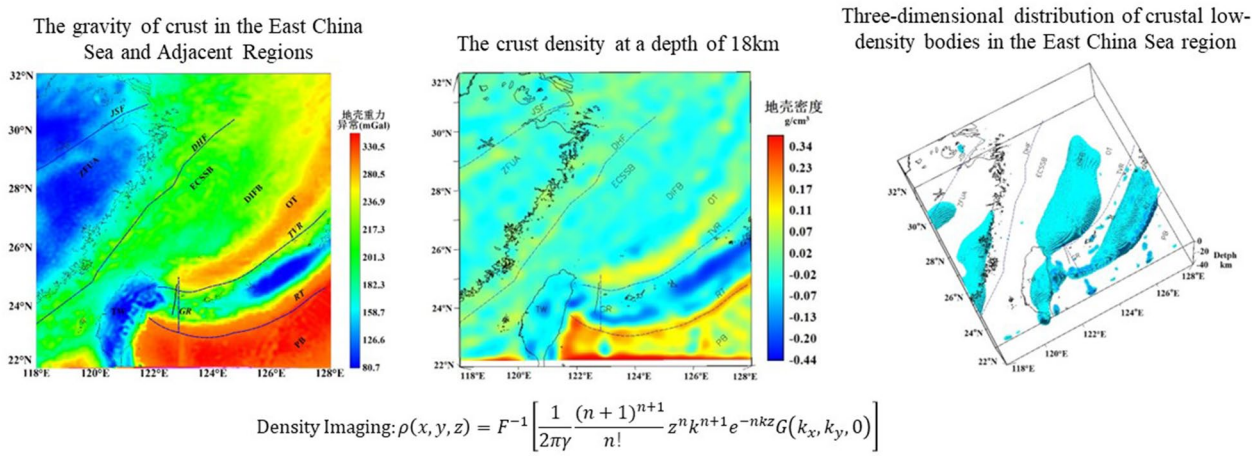

Introduction

The East China Sea stretches eastward from the Chinese mainland to Japan's Kyushu Island and the Ryukyu Islands, serving as an important maritime region in eastern Asia and providing a significant window into the formation and evolution of the West Pacific marginal sea's tectonics. This region is located at the boundary of the Eurasian, Philippine Sea (PB), and Pacific tectonic plates, where the relative movement of these plates causes tectonic processes such as crustal collisions, subduction, and compression (Suo et al. 2020; Corchete 2022) (Fig. 1a). Consequently, the geography of the region is diverse and complicated, with numerous islands, sandbanks, seabed ridges, and seamounts. The geological structure involves a variety of geological phenomena, including plate motions, volcanic activity, faults, and uplifts, which provides geologists and geophysicists with abundant research opportunities. Exploration and research of deep structural characteristics and crustal density distribution in this region provide scientific evidence and data support for a comprehensive knowledge of geological history

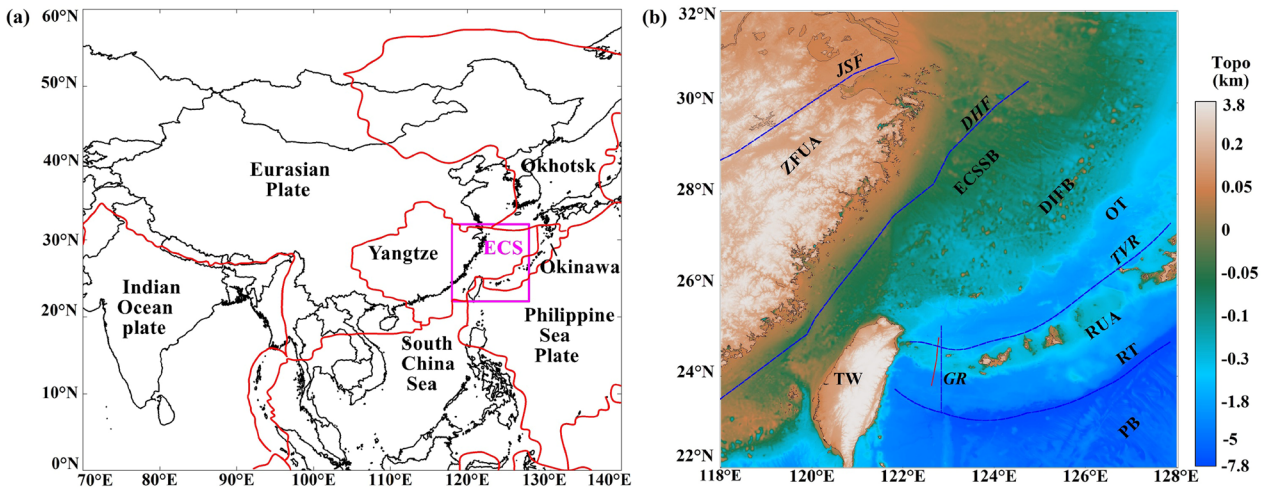

Fig. 1 Location of the study area and topography in the East China Sea and adjacent regions (Gao et al. 2008a, b; Shang 2014; Yang et al. 2018; Minami et al. 2022; Bird 2003). **a** Location of the study area. **b** Topographic map from STRM15 (Tozer et al. 2019). The red line is the plate boundary line and the purple box the study area. *ECS* East China Sea, *ZFUA* Zhejiang-Fujian Uplift Area, *ECSSB* East China Sea Shelf Basin, *DIFB* Diaoyu Islands Folded Belt, *OT* Okinawa Trough, *RUA* Ryukyu Uplift Area, *PB* Philippine Basin, *DHF* Dongyin-Haijiao Fault, *JSF* Jiangshao Fault, *TVR* Tokara Volcanic Ridge, *RT* Ryukyu Trench, *GR* Gagua Ridge, *TW* Taiwan

and geodynamic evolution. It also serves as a valuable resource for seismic disaster prevention, resource exploration, marine environmental preservation, and maritime security in this region (Wang et al. 2023; Yang et al. 2018).

As the Pacific plate moves in different ways at different times and in different regions, the East China Sea and its neighboring areas have formed a tectonic pattern of east–west zoning and north–south zoning. The east–west zoning is the basic feature of tectonic movements in the sea, from west to east, from old to new, mountain building and basin building movements, all migrating eastward, with continents continually accreting into the ocean. The East China Sea and its neighboring areas show the characteristics of "three rises and two basins", which are, from west to east: the Zhejiang-Fujian Uplift Area (ZFUA), the East China Sea Shelf Basin (ECSSB), the Diaoyu Islands Folded-uplift Belt (DIFB), the Okinawa Trough Basin (OT) and The Ryukyu Uplift Area (RUA) (Fig. 1b). This region has been subjected to several tectonic processes, resulting in a complicated geological structure. Aside from the development of north–northeast-oriented faults that divide the region into eastern and western belts, the area also exhibits characteristics of north–south block motions, which influence sedimentation and hydrocarbon accumulations. The ECSSB is a vast underwater basin with a fan-shaped or pan-shaped morphology (Zhang et al. 2022; Cheng et al. 2023). It is a Cenozoic extensional basin characterized by sag-type basins superimposed over graben-type basins, such as the western graben, central low uplift, and eastern graben (Lin et al. 2005). The region is dominated by many fault structures, with each geological unit consisting of various depressions or uplifts, all of which contribute to the ECSSB's complex geological morphology (Chen et al. 2013; Yang et al. 2022; Zhang and Zhang 2015). The DIFB is a north–northeast to northeast–northeast-trending arc-shaped uplift located between the ECSSB and the OT. The OT Basin, located to the east of the DIFB, has a similar arc-shaped distribution with a north–northeast trend. It is a relatively deep submarine basin characterized by an east–west orientation and a longer north–south reach (Sibuet et al. 2021). The basin floor is relatively flat, with several higher seabed ridges and seamounts surrounding it (Nishizawa et al. 2019). The joint motion of the Eurasian Plate, Philippine Sea Plate, and Pacific Plate influences the East China Sea region. Various deformation motions such as plate subduction and compression occur at the intersection of these plates, causing crustal subsidence and compression and changes in the geological morphology and structure of the East China Sea region. Crustal density, which reflects the composition and tectonic features of the crust, is critical for understanding the distribution of crustal structures and further assessing the geotectonic processes in the area.

The density structure of the crust is an important characteristic for understanding its interior composition (Carlson and Raskin 1984). Direct geological drilling methods, however, are difficult and expensive, particularly in deep-sea areas. As a result, scientists have sought indirect methods to investigate and research the structure and properties of marine crusts, such as seismic reflection and refraction, gravity, and magnetic field surveys (Bai 2014). Gravity data collecting is the simplest and least expensive of these geophysical approaches, making it an important strategy for understanding marine crustal density structures. Furthermore, as modern computer and geophysical data processing technology has advanced, this approach has gained substantial improvements in resolution and accuracy. Gravity measurements are widely utilized in geophysical research to indicate the distribution of subsurface densities since the strength of the gravity field is directly related to material density. Gravitational anomalies induced by all density fluctuations within the crust, including those associated with the crust–mantle boundary and finer interior structures, provide precise information about the crust. To obtain the density distribution inside the marine crust, three-dimensional (3D) density structure inversion based on gravity data is used (Fei et al. 2018). Density fluctuations can be determined by examining changes in the gravity field induced by the crust, providing insights into the internal structure and evolutionary history of marine crusts.

Gravity data inversion methods typically rely on gravity data collected from marine observations or satellites. However, some substantial obstacles remain in the inversion research of marine crustal density structure. First, there are limitations in data quality and quantity. Gravity data in marine environments are often difficult to obtain and may not completely cover the region, which might affect inversion results. Data collecting becomes more difficult, especially in deep-sea and remote regions. In addition, due to the complexity of the marine environment, gathered data may contain noise and hence require sophisticated preprocessing before being appropriate for inversion (Johnson et al. 2000; Radhakrishna et al. 2010; Chen et al. 2019). Moreover, the complexity and ambiguity of inversion models pose difficulties. Inversions of marine crustal density structures often require a large number of parameters, making the problem highly complex. Due to the complexity of the crust and the non-uniqueness of the inversion problem, multiple models can describe the same set of data, forcing the development of more sophisticated optimization algorithms and constraints to reduce model uncertainty. Finally, significant

computational resources are necessary. Inversion of marine crustal density structure sometimes necessitates a substantial amount of computer resources, posing a challenge for research teams without robust computing capabilities. The computational needs become increasingly substantial when working with a high number of model parameters or processing considerable amounts of data. Nonetheless, with technological advancements, gravity field data obtained from satellites, aircraft, and ground sources have become increasingly sophisticated and higher in resolution. These high-quality data provide more accurate inputs for crustal density structure inversion (Yu et al. 2023). In terms of inversion methods, in addition to traditional gravity inversion methods, more research has begun to investigate new inversion approaches and utilize multiple geophysical data for joint inversion to produce more comprehensive and accurate results. Fei et al. (2018) have used gravity inversion combined with seismic results to obtain new information on the 3D density structure of the Ross Sea. An adaptive weight function of the density inversion method has been proposed for density inversion with gravity data (Li et al. 2022). Equivalent source inversion has been introduced into the density inversion to obtain the 3D density structure of the East China Sea region consistent with seismic results (Petrishchevsky 2022). These research trends demonstrate that in the future, the use of new technology and methods will gradually revolutionize the study of marine crustal density structure inversion, making it more sophisticated, comprehensive, and useful. However, for data of large regional scope, these methods exhibit the disadvantage of computational redundancy.

Addressing today's challenges requires multifaceted responses. To begin, it is critical to develop a high-precision global gravity field model. Increasing measurements and updated satellite gravity data contribute to constructing high-resolution global gravity field models. Satellite gravity data are invaluable, particularly for global marine regions. However, because the oceans encompass 70% of the planet, both gravity forward and inverse systems require rapid and efficient qualities. In this context, conventional spatial domain inversion approaches have obvious limitations. In contrast, the wavenumber domain 3D density imaging method converts gravity model forward calculations to the wavenumber domain, simplifying operations through simple multiplication and division and avoiding complex convolution and deconvolution calculations typical of spatial domain inversion methods (Cui and Guo 2019). This greatly increases imaging speed. Furthermore, the wavenumber domain approach can better handle high-frequency data, improving imaging resolution. It can produce density models with high resolution and accuracy using depth restrictions and continuous iterations. Therefore, the wavenumber domain 3D density imaging method has substantial advantages in studying the density structure of the marine crust.

Gravity anomalies in the East China Sea

As satellite observation technology continues to advance, the availability of high-sensitivity and high-precision satellite gravity data covering the entire globe has become instrumental in the meticulous analysis of Earth's density distribution. The utilization of high-precision gravity data, in particular, offers cost-effective advantages for scrutinizing the internal structure of the Earth, particularly in oceanic regions (Fei et al. 2018). In this study, we collected high-precision topography and gravitational anomaly data from the East China Sea region. The topographic data were sourced from SRTM15 (Shuttle Radar Topography Mission), boasting a spatial resolution of 15"×15" and an accuracy of approximately 0.5 km (Tozer et al. 2019). This dataset comprised both land elevation and ocean depth data. The ocean depth data, generated through a meticulous fusion of more than 33.6 million ship surveys and satellite altimetry predictions, provided a comprehensive representation of the underwater landscape. Land data, including elevation, were extracted from previously published digital elevation models. The free-air gravity data employed in our analysis were derived from the high-resolution Earth Gravity Anomaly Model WGM2012 with a spatial resolution of 1'×1' (Bonvalot et al. 2012). The Bouguer gravity anomalies were from SGG-UGM-2, which was described by Liang et al. (2020). The new model was a High-Resolution Earth's Gravity Field Model from GOCE, GRACE, Satellite Altimetry, and EGM2008, up to degree 2190 and order 2159. The recorded gravity statistics effectively captured fluctuations in Earth's density. To ensure accuracy, field separation was imperative to extract gravity anomalies induced by density variations in the crust. Furthermore, within the research area, additional data from CRUST1.0 about sediment layers (Laske et al. 2013), Moho depth data (He et al. 2019), and low-order gravity field data (Fang 2002; Liang et al. 2020) were meticulously gathered. These datasets played a crucial role in mitigating the gravity anomalies produced by crustal density heterogeneity. Subsequently, we employed a wavenumber domain 3D density imaging approach to invert the crustal density distribution in the region. This methodology allowed for a comprehensive understanding of the subsurface structures in the East China Sea region.

The gravity anomalies in the East China Sea region have distinctive characteristics. The ECSSB's free-air gravity anomaly fluctuates gradually and primarily goes northeast (Fig. 2a). The DIFB's free-air gravity anomaly

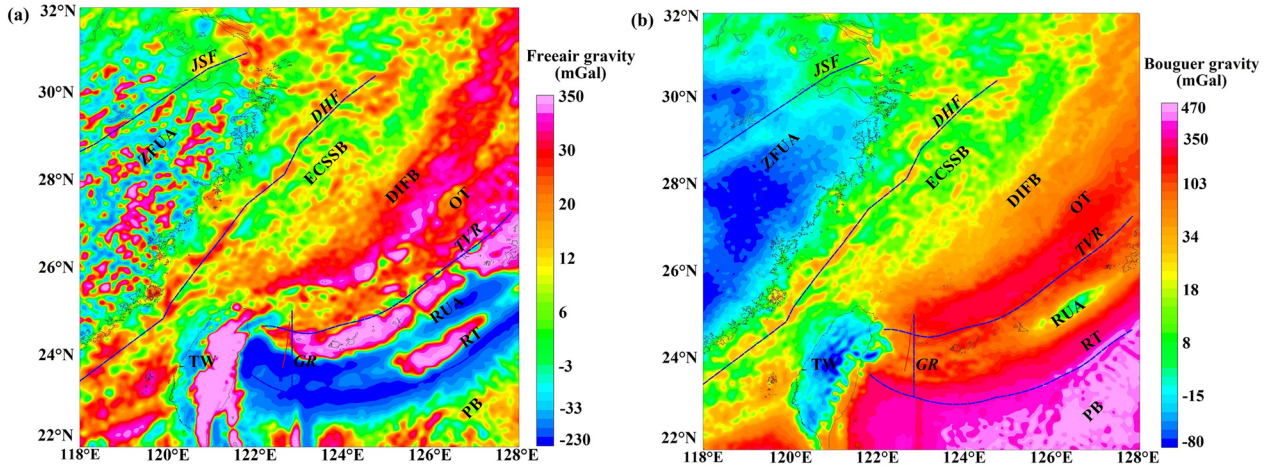

Fig. 2 Gravity anomalies in the East China Sea and adjacent regions. **a** Free-air gravity anomalies, from the WGM2012 global gravity model (Bonvalot et al. 2012). **b** Bouguer gravity anomalies, from SGG-UGM-2 (Liang et al. 2020)

has a north–eastward trend with increasing anomaly gradients. The free-air gravity anomaly changes slowly in the southern half of the OT Basin, whereas it fluctuates significantly in the northern part. Gravity anomalies are primarily caused by the evolution of deep structures. The amplitudes of the anomalies increase progressively from northwest to southeast, indicating a slow uplift of the Moho depth. The Bouguer gravity anomaly in the ZFUA of China steadily increases from west to east, changing from negative to positive (Fig. 2b). The negative anomaly trend coincides with the coastline, trending northeast, and interacts with positive anomalies in the nearby offshore locations, demonstrating that continental gravity anomalies extend into the sea. The ECSSB Bouguer gravity anomaly primarily exhibits a mild northeastward trend with positive anomalies. The Bouguer gravity anomaly begins to increase in the DIFB area on the eastern side of the ECSSB, establishing a north–northeast to north–east–northeast-trending zone of high anomalies in the OT, indicating a somewhat thinner crust in the OT compared to the surrounding areas.

Gravity anomalies are comprehensive reflections of inhomogeneous subsurface materials (Gao et al. 2000). To extract the gravity anomalies induced by crustal density fluctuations, sediment layers (Ding 2004; Xu 2020), the Moho interface (He et al. 2019), and the Earth's low-degree gravity field contributions were eliminated from the Bouguer gravity anomalies (Fang 2002; Liang et al. 2020).

The difference between the observed Bouguer gravity anomaly (g_{obs}) and the contributions from sediment layers (g_{Sedi}) (Fig. 3a), the Moho interface (g_{Moho}) (Fig. 3b), and the Earth's low-degree gravity field (g_{GE}) (Fig. 3c) was used to determine the residual gravity anomaly (g_{residual}):

$$g_{\mathrm{residual}} = g_{\mathrm{obs}} - g_{\mathrm{Sedi}} - g_{\mathrm{Moho}} - g_{\mathrm{GE}}. \quad (1)$$

This process allowed us to acquire gravity anomalies caused mostly by crustal density fluctuations. We could gain valuable insights into the crustal structure and tectonic aspects of the East China Sea area by analyzing these residual gravity anomalies.

The gravity anomalies predominantly caused by crustal density variations in the East China Sea region were obtained after the successive elimination process (Fig. 3d). Gravity anomalies in the ZFUA are characterized primarily by modest low values. In the central section, a prominent northeast-trending anomaly belt coincides with the Jiangshao Fault (JSF), indicating crustal thinning and Moho elevation (He et al. 2019; Shang et al. 2017; Zhu et al. 2022).

The gravitational anomalies over the ECSSB are generally moderate. The high-value gravity anomaly closure corresponds to the northeast-trending Dongyin-Haijiao Fault (DHF) on the western side of the ECSSB. Gravity anomalies begin to rise on the eastern side of the ECSSB, in the DIFB region, forming north–northeast to northeast-trending high-value anomaly belt, indicating a substantially thinner crust in the OT basin compared to the surrounding regions. This is most likely owing to the impact of the collision between the Philippine Sea Plate and the Pacific Plate, which resulted in the formation of crustal morphology orientated north–northeast to northeast. The bathymetric map (Fig. 1b) depicts relatively flat terrain at the basin's bottom.

The elongated ridges of the Tokara Volcanic Ridge (TVR) on the eastern side of the OT correspond well

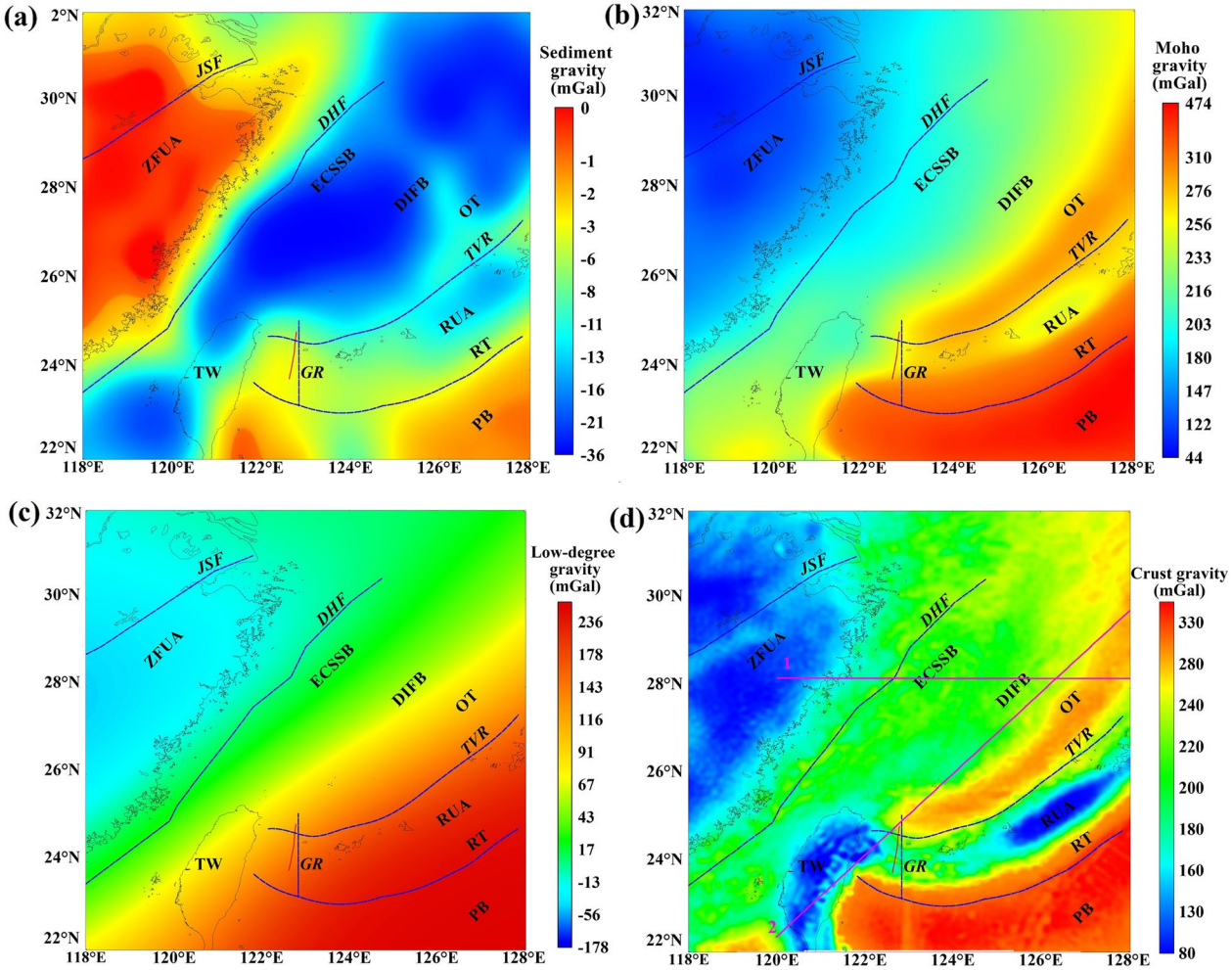

Fig. 3 Gravity anomalies caused by different factors in the East China Sea and adjacent regions. **a** caused by sedimentary layers **b** by Moho **c** 2-60th order gravity field low-degree terms **d** by crustal density differences. Profiles 1 and 2 were previously studied (Petrishchevsky 2022)

to the gradient band of the crustal gravity anomaly. The Ryukyu Trench (RT) region has relatively low gravity anomalies, generating a distinct depression between the high-value gravity anomalies on both sides, indicating crustal thickening. Gravity anomalies in the area around Taiwan are typically characterized by low values, in sharp contrast to the high-value zone associated with the Philippine Sea Plate. The presence of a thin oceanic crust in this region is reflected by a widespread high gravity anomaly on the Philippine Sea Plate.

Wavenumber domain density imaging method for inverting crustal density in the East China Sea and adjacent regions

The wavenumber domain 3D density imaging method is a straightforward approach for calculating subsurface density distributions based on gravity anomalies in the wavenumber domain (He 2022; He et al. 2024). Previous researchers suggested the Cribb imaging approach, which utilized the Fourier transform to compute the subsurface density distribution by analyzing the vertical derivatives of recorded gravity anomalies (Cribb 1976). Kobrunov (2015) introduced a density equivalence distribution method that converts gravity data into the wavenumber domain using a rapid Fourier transform. This approach inversed the density distribution based on the gravity data spectrum and refined the density equivalency distribution further using functional representation, resulting in the quick development of subsurface density distribution and structural models. To optimize this strategy, subsequent researchers incorporated previous information and used stochastic iteration (Kobrunov and Varfolomeev 1981; Priezzhev et al. 2014). By recognizing extreme points, the Depth from Extreme Point (DEXP) imaging method predicted the depth of anomalous bodies (Fedi 2007), which was a fast and stable approach.

Building upon prior research, Cui and Guo (2019) added a depth ratio component to the wavenumber domain iterative method for rapid potential field imaging employing gravity anomalies and their gradients, resulting in high-resolution and accurate density models. The wavenumber domain density imaging method, which was based on high-precision gravity field model data, efficiently tackled data quality and computational resource issues in gravity inversion for the density structure of the oceanic crust. Moreover, because this strategy did not rely on priori models, it was especially important for marine locations with low prior data support.

Previous research (Priezzhev et al. 2014) has found that the density imaging formula in the wavenumber domain can be represented as follows:

$$\rho(x,y,z) = F^{-1}\left[\frac{1}{2\pi\gamma}\frac{(n+1)^{n+1}}{n!}z^n k^{n+1} e^{-nkz} G(k_x,k_y,0)\right], \tag{2}$$

where F^{-1} is the Fourier inverse transform, $G(k_x,k_y,0)$ represents the spectrum of the gravity anomaly spectrum, γ is 6.67×10^{-11} N m^2/kg^2, which is the gravitation constant, k_x and k_y are the wavenumbers along the x-and y-axes, respectively. The constant n $(1<n<10)$ represents the resolution of the filter, with larger values signifying higher resolution. z is the inversion depth, k is the wavenumber, $k=\sqrt{{k_x}^2+{k_y}^2}$, and ρ is the density of the mass body at a given point. The wavenumber domain density imaging method's efficacy and resilience have been rigorously tested using forward model inversion and noisy data (He et al. 2024). A depth weighting function was incorporated to improve vertical resolution even further (Commer 2011).

$$W(z) = \frac{\alpha+\exp\left[\frac{d_1}{dz}(z-z_{c1})\right]}{1+\exp\left[\frac{d_1}{dz}(z-z_{c1})\right]} - \frac{\alpha+\exp\left[\frac{d_2}{dz}(z-z_{c2})\right]}{1+\exp\left[\frac{d_2}{dz}(z-z_{c2})\right]}, \tag{3}$$

where dz is the inversion domain, α is an empirical value that determines the weights at the near-surface, $\alpha=0.001$(Commer 2011), z_{c1}, z_{c2} are the depths of the top and bottom depths of the model. d_1 is the interface constraint factor for the upper interface and d_2 the interface constraint factor for the lower interface. The iterative inversion equation with depth weighting function is shown below:

$$\rho_{i+1} = \rho_i + W(z)\times\Delta\rho_i, \tag{4}$$

where ρ_{i+1} is the density distribution at $i+1$ iteration, ρ_i is the density distribution at i iteration, and $\Delta\rho_i$ is the density correction.

The inverted subsurface domain is divided into N horizontal levels, each of which is further segmented into $m\times n$ orthogonal prisms. The following is the iterative procedure for each prism within the geological layers. This information-independent approach enables direct initialization of density values to zero (Fig. 4). For specific steps and model validation, please refer to the author's doctoral thesis and the journal paper (He 2022; He et al. 2024).

Crustal density characteristics in the East China Sea and adjacent regions

Based on the crustal gravity anomalies, the wavenumber domain 3D density imaging technique was used in this study. Given that the maximum depth of the Moho discontinuity in this location was inferred to be 33 km (He et al. 2019), the depth for density inversion was set at 38 km, with 1 km spacing between inversion depths, and a total of 50 iterations were performed. Figure 5 depicts the results of crustal density perturbations in the East China Sea region. The gravity anomaly residuals from forward gravity anomaly separation had a standard deviation of 34 mGal.

At a depth of 2 km (Fig. 5a), the inversion results reveal that shallow regions have somewhat indistinct density variations, mostly centered around zero values, indicating effective gravity anomaly separation. Density differences are especially pronounced near the eastern edge of Taiwan and the RT (Yang et al. 2008). Density fluctuations within the upper crust reveal a modest increase at 6 km depth (Fig. 5b) as compared to the 2 km depth slice, with

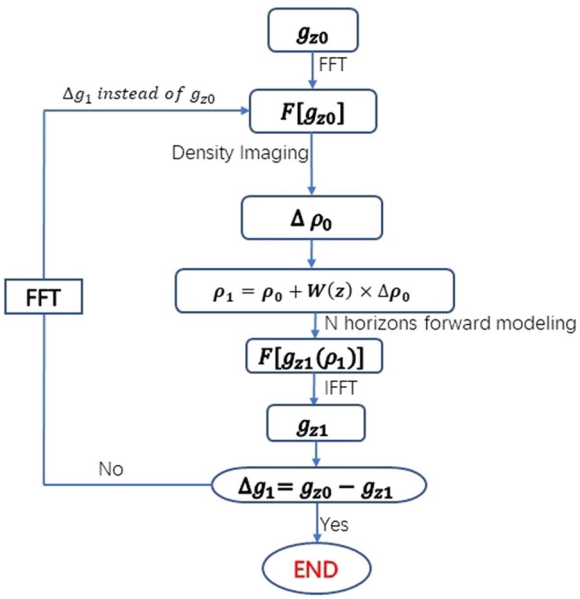

Fig. 4 Flowchart of the wavenumber domain 3D density imaging method, ρ_0 is the initial density, which can be set to 0. A great advantage of this method is that it does not depend on a priori information. $w(z)$ is the depth constraint factor in formula (3)

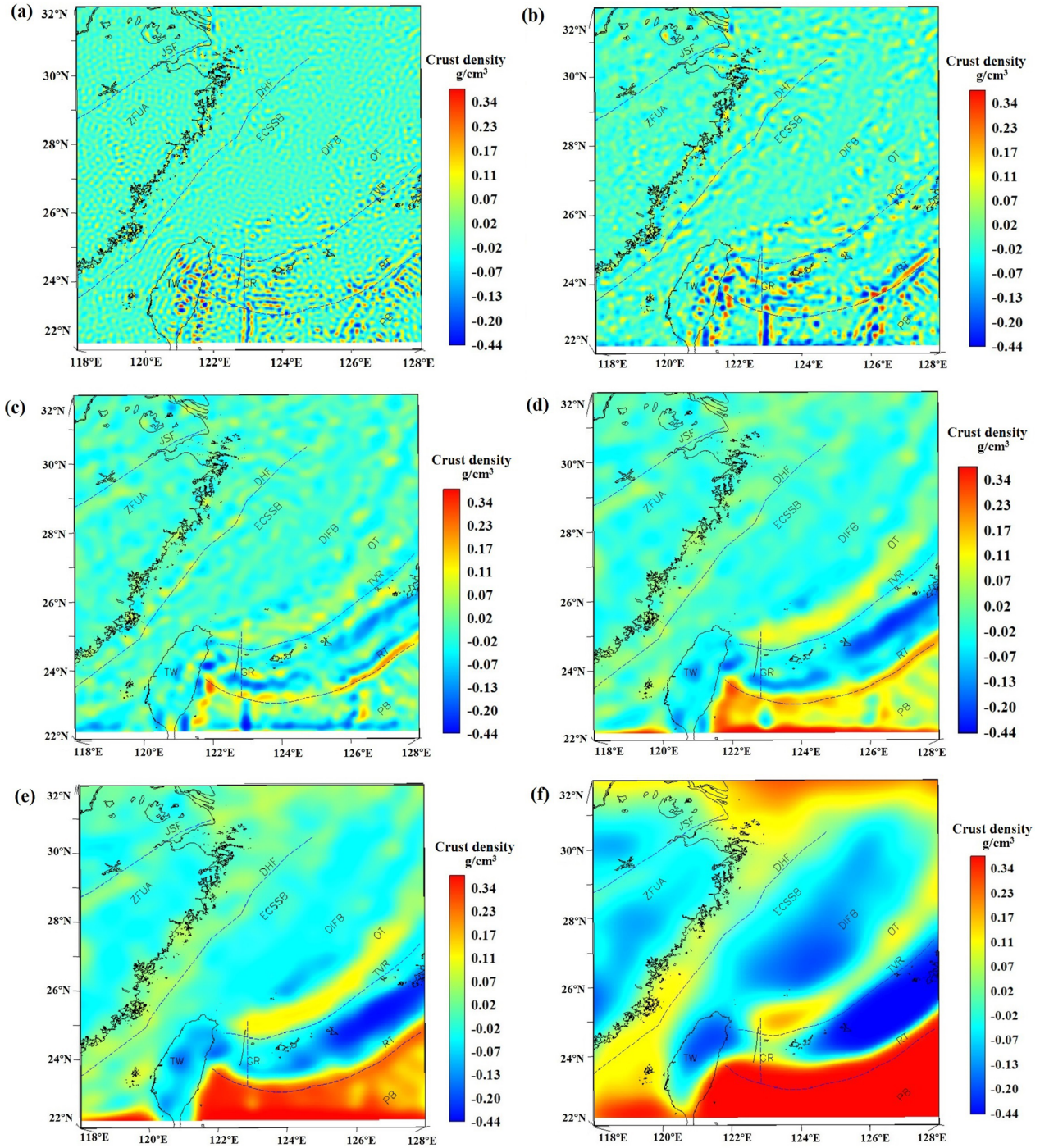

Fig. 5 Depth slices of crustal density disturbance distribution in the East China Sea and adjacent regions. **a** 2 km, **b** 6 km, **c** 12 km, **d** 18 km, **e** 25 km, **f** 38 km

prominent northeast-oriented banding characteristics. Notably, the DHF is visible, surrounded by some beaded anomaly. The fault is less apparent in the 2 km depth slice, but it becomes more visible in the 6 km depth slice. The ECSSB displays overall minor variations with smaller anomalies in the northeast-oriented bands. The OT Basin exhibits a trend of changing anomalies, with variations orientated northeast and north–northeast. A significant northeast-oriented positive anomaly belt is detected in the RT, whereas a north–south-oriented negative

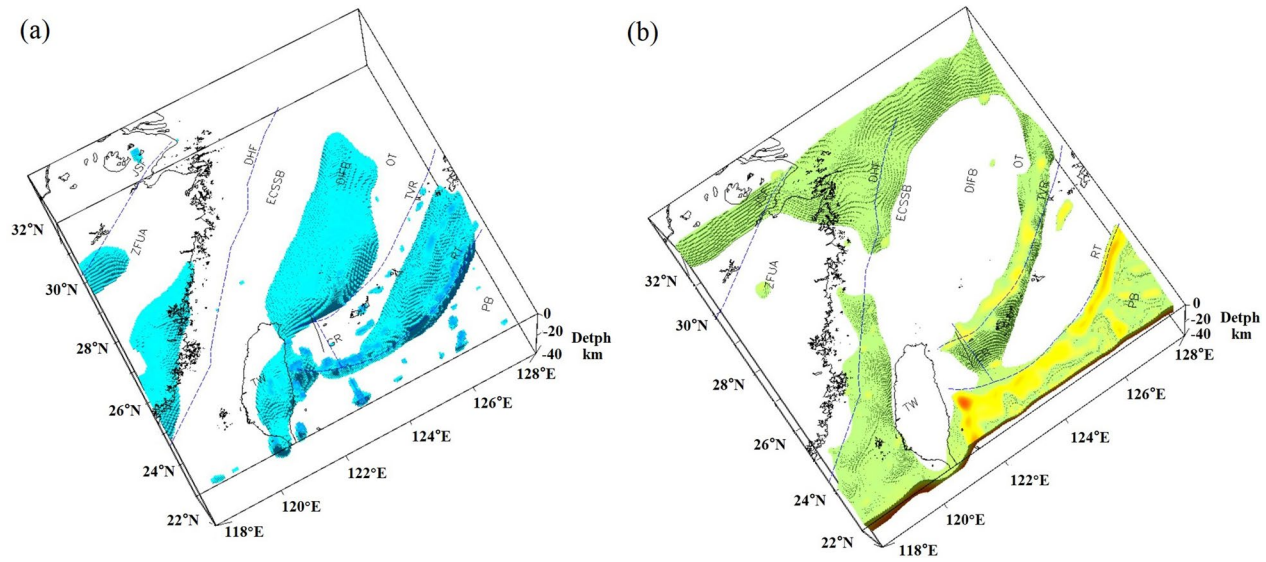

Fig. 6 3D map of crustal density distribution in the East China Sea and adjacent regions. **a** Negative density,$\sigma < -0.1\ \mathrm{g/cm^3}$. **b** Positive density, $\sigma > 0.6\ \mathrm{g/cm^3}$

anomaly belt develops to the south of the Gagua Ridge (GR).

The smaller high-value anomaly closures observe in the shallow crustal density perturbations gradually diminish at a depth of 12 km (Fig. 5c). The extent of density perturbation anomalies increases, and distinct discontinuous anomaly closures are apparent near the JSF and DHF. These observations indicate that the development depth of these two faults is within the crust. The central part of the ECSSB still exhibits relatively moderate density perturbations, with low anomaly magnitudes. The DIFB exhibits a negative anomaly belt trending north–northeast to northeast, in contrast to a positive anomaly belt trending in the same direction in the OT. The RUA has noticeable low negative anomaly features, and the Moho interface inversion data show extensive subsidence in this area, reaching depths of up to 26 km, indicating substantial crustal thickness (He et al. 2019). The positive anomaly belt of density perturbations in the RT is more pronounced, largely coinciding with the trench. The Moho interface rapidly ascends in this region, reaching a height of 9 km below the PB. Within the arc basin crust, there are significant density perturbation anomalies. The trench and the PB exhibit high-density perturbations, indicating the higher positive and negative density perturbations induced by mass compensation discrepancies beneath the high-density and low-density zones beneath the RUA.

At a depth of 18 km (Fig. 5d), density perturbations in the ECSSB demonstrate a smooth and expanded range of low-negative values, whereas density perturbations in the trench–arc basin region show an increasing disparity. The TVR and the RT form a north–northeast to northeast-trending positive anomaly band in the OT region. In the RUA, density perturbations correspond to a low-negative value area, whereas in the PB, density perturbations indicate a northwesterly-trending positive high-value anomaly. These observations indicate an uneven distribution of resources in this region (Dai 2004). The Moho discontinuity, which ranges from 26 to 28 km in the ECSSB, is raised to its shallowest position in the OT at 21 km, while the Moho in the RUA subsides again, reaching its lowest depth at 26.4 km (He et al. 2019). The density perturbations inside the crust move from a low-negative value mild zone to high-positive value anomaly bands, illustrating the transition of crustal characteristics in this location from continental to transitional. The PB's Moho is significantly elevated and denser than the trench–arc basin region, displaying typical oceanic crust features with high-density mantle compensating material beneath.

At a depth of 25 km (Fig. 5e), the density perturbations in the ZFUA and the ECSSB indicate negligible variations in the Moho discontinuity, indicating limited alterations in this region. Density perturbations remain visible in the trench–arc basin area, with the OT Basin exhibiting distinct north–northeast to northeast-trending positive high-value anomaly bands. The TVR and the RT flanking the RUA are nicely aligned with the nearby high-density perturbation gradient band.

At a depth of 38 km (Fig. 5f), west of the RT, the density perturbation pattern is generally consistent with mostly

low negative values, whereas the Philippine Sea Plate presents a variety of positive high values. This discrepancy reflects the differing nature of the plate on both sides of the RT, implying heterogeneous upper mantle material distribution in the East China Sea arc basin, which is likely due to the joint effect of the Philippine Sea Plate and the Eurasian Plate. In the subduction zone, the distribution of oceanic and continental crusts may be mixed, resulting in complex contact connections at various depths.

The 3D display of crustal density distribution in the East China Sea region depicts the negative and low-density perturbations in the ECSSB and the RUA more intuitively (Fig. 6a). These perturbations are most likely caused by the predominance of sedimentary and volcanic rocks in the ECSSB's crust. Furthermore, tectonic activities such as fault zones and mantle upwelling may have an impact on the region, contributing to the reduction in crustal density. The crust west of the DHF displays predominantly negative low-density anomalies. The OT and the PB, in contrast, are characterized by positive high-density perturbations with density anomaly bands that closely mimic the TVR (Fig. 6b).

In this study, we extracted two profiles (Profiles 1 and 2 in Fig. 3) from the 3D density structure generated using gravity inversion. Both profiles traversed the

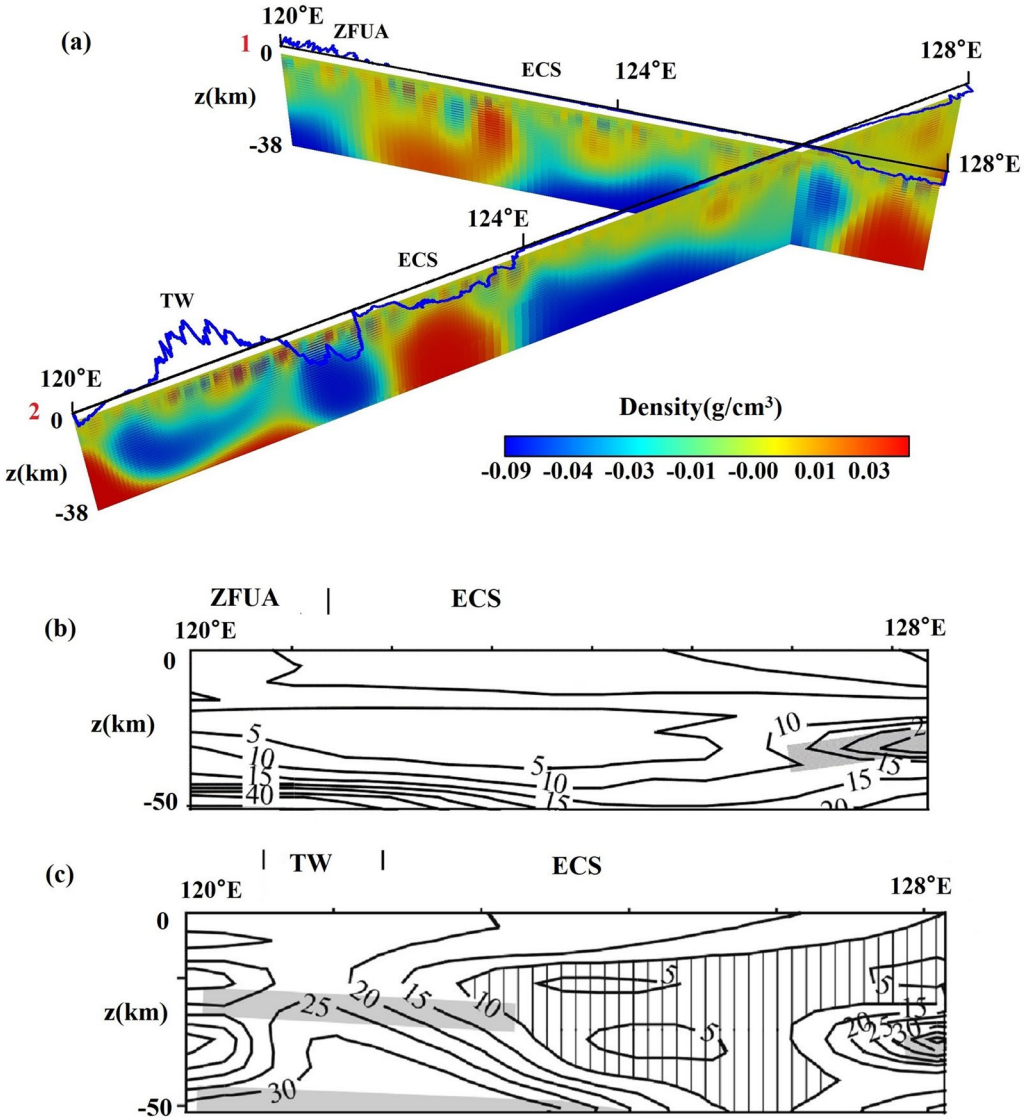

Fig. 7 The density of Profiles 1 and 2 in Fig. 3, **a** the profiles were extracted from the result of this work. **b**, **c** Density contrast isolines, $\times 10^{-2}$ kg/m^3, they were revised from previously studied (Petrishchevsky 2022)

ECSSB (Fig. 7). Profile 1 was oriented east–west, beginning at the ZFUA, and continuing through the ECSSB, DIFB, and OT. Profile 2, on the other hand, was oriented northeastward, beginning from the southwest side of TW and stretching across TW, crossing the ECSSB, and continuing into the DIFB and OT. The two density profiles extracted in this study provide a more detailed representation of density fluctuations along the surveyed transects. Profile 1 shows a rather progressive shallow disturbance eastward of the ZFUA. However, there is a notable growing tendency in density perturbations in the direction of the ECSSB, peaking near the position of the DHF. The density perturbations tend to stabilize on the eastern side of the fault, correlating with previous research findings (Fig. 7b). This observation indicates a transition from continental crust to transitional crust on both sides of the DHF. Moreover, there is a significant increase in density perturbations below the depth of 20 km from the east to the OT. This observation implies the occurrence of mantle upwelling in the region, resulting in a density increase, which is consistent with previous studies. Profile 2 shows only minor density disturbances beneath Taiwan Island, indicating relative crustal stability in this region. The Moho surface inversion data indicate that the Moho depth beneath Taiwan is deeper than 30 km, which is typical of continental crust. Moving northeastward, the density perturbation diminishes first, then increases, with the boundary of this change closely aligned with the RT and TVR positions. This suggests that the region has seen significant crustal deformation as a result of the collision of the Indian and Eurasian plates, resulting in complicated fluctuations in crustal density disturbances. The fluctuations in density detected in the OT are consistent with earlier research, with all values falling within the low-density zone, indicating typical oceanic crustal characteristics (Petrishchevsky 2022).

Further analysis is conducted to uncover the deep structural evolution in this area based on the crustal density distribution in the East China Sea region, in conjunction with the Moho interface inversion results and geological data. The East China Sea region represents a complex plate boundary with subduction processes involving the Eurasian Continental Plate, the Philippine Sea Plate, and the Pacific Plate, resulting in structural consequences such as crustal collision, subduction, and compression (Corchete 2022; Liu et al. 2022). The Pacific Plate and the Philippine Sea Plate subduct northwestward relative to the Eurasian Continental Plate in the East China Sea region. When these large oceanic plates converge with the Eurasian Continental Plate, considerable subduction occurs along the plate boundaries. In the subduction zone, the mixing distribution of oceanic and continental crusts produces intricate patterns of mantle material. Subduction generates crustal subsidence and compression, which results in morphological and tectonic changes in the East China Sea region, such as uplift, subsidence, horizontal compression, and extension. From the ZFUA continental crust to the ECSSB, through the OT and the RUA transition zones with oceanic crust, and eventually to the PB with oceanic crust. The tectonics of the East China Sea trench–arc–basin system are the result of the interaction between continental and oceanic plates via subduction and are intimately tied to crustal uplift and subsidence. Other structures in the region, such as the RT and the GR, are associated with crustal extension. In addition, plate subduction may cause mantle magma upwelling and volcanic eruptions, contributing to the East China Sea region's active volcanic activity.

Conclusion

This study delved into the crustal density structure of the East China Sea and surrounding regions, inverting the crustal density distribution using the wavenumber domain 3D density imaging method with high-precision global satellite gravity data. We have gotten a better understanding of the geological history and geodynamic development of this region by investigating crustal density structure. This provided essential references for earthquake disaster prevention, resource exploration, marine environmental preservation, and maritime security.

However, several challenges were encountered during the process of marine crustal density structure inversion including constraints in data quality and quantity, complexity and uncertainties in inversion models, and the need for significant computer resources. In the future, with the development of next-generation satellite gravity measurement missions and developments in wavenumber domain inversion techniques, we should expect to obtain higher precision and more extensive marine crustal density structure inversion results.

The wavenumber domain 3D density imaging method revealed substantial advantages in this study, overcoming limitations in data quality and computational resources, while also presenting a novel research tool for the investigation of marine crustal density structure. The crustal density distribution results showed density fluctuations and anomaly distributions at different depths, revealing the East China Sea region's complex and diversified geological processes and crustal changes. Particularly, the negative and low-density perturbations observed in regions such as the ECSSB and the RUA may be attributed to the ECSSB's predominant presence of sedimentary and volcanic rocks. In addition, tectonic activities

such as fault zones and mantle upwelling may further contribute to the region's crustal density decline.

In conclusion, our study has provided scientific evidence and data support for a deeper understanding of the geological and geodynamic processes in the East China Sea and adjacent regions through the inversion of crustal density structure. Future research should continue to refine inversion methods, enhance data quality control, and incorporate additional geological information to obtain more accurate and comprehensive marine crustal density structure information. This will facilitate further exploration of the crustal evolution processes and mechanisms in the East China Sea and surrounding areas, offering more trustworthy foundations for scientific research and applications in related disciplines.

Acknowledgements
This work was financially supported by the National Natural Science Foundation of China (Grant No. 42192535), the Open Fund of Wuhan, Gravitation and Solid Earth Tides, National Observation and Research Station (No. WHYWZ202204), the Strategic Pioneer Science and Technology Special Project of the Chinese Academy of Sciences (Grant No. XDB18010304), and the National Natural Science Foundation of China (Grant No. 41874096). We are grateful to the editors and reviewers for their constructive comments and suggestions, which have helped us improve the manuscript. Thanks are extended to the entire Division of Seismology and Physics in the Earth's Interior team at the Innovation Academy for Precision Measurement Science and Technology.

Author contributions
HH: conceptualization, methodology, investigation, formal analysis, writing—original draft; HS: supervision, project administration; JF: funding acquisition, supervision, writing—review and editing; DG: conceptualization; JL: data curation.

Data availability
The topographic data are from SRTM15_PLUS, which is a data fusion of SRTM land topography with measured and estimated seafloor topography, archived by Tozer et al. (2019) at https://topex.ucsd.edu/pub/srtm15_plus/. The Free-air gravity anomalies are described by Bonvalot et al. (2012) at https://bgi.obs-mip.fr/data-products/grids-and-models/wgm2012-global-model/. The Bouguer gravity anomalies are from SGG-UGM-2, which are described by Liang et al. (2020) at https://doi.org/10.1016/j.eng. 2020.05.008. The sediment layers' data are from CRUST1.0, which is archived by Laske et al. (2013) at https://igppweb.ucsd.edu/~gabi/crust1.html, and the Moho interface is archived by He et al (2019) at https://doi.org/10.13203/j.whugis20170330, and the Earth's low-degree gravity field is the same with the Bouguer gravity anomalies.

Declarations

Competing interests
The author(s) declare(s) that they have no competing interests.

Author details
[1]State Key Laboratory of Geodesy and Earth's Dynamics, Innovation Academy for Precision Measurement Science and Technology, Chinese Academy of Sciences, 340 Xudong Road, Wuhan 430077, China. [2]Wuhan Gravitation and Solid Earth Tides National Observation and Research Station, Wuhan 430071, China. [3]University of Chinese Academy of Sciences, No. 19A Yuquan Road, Beijing 100049, China.

Received: 26 September 2023 Accepted: 5 January 2024
Published online: 25 January 2024

References

Bai Y (2014) Lithosphere Density Modeling Based on Multi-Source Gravity: Methods and Applications Ph.D., China University of Petroleum Doctoral Dissertation
Bird P (2003) An updated digital model of plate boundaries. Geochem Geophys Geosyst. https://doi.org/10.1029/2001gc000252
Bonvalot S, Balmino G, Briais A, Kuhn M, Peyrefitte A, Vales N, Biancale R, Gabalda G, Reinquin F, Sarrailh M (2012) World Gravity Map. Commission for the Geological Map of the World. Eds. BGI-CGMW-CNES-IRD, Paris. https://doi.org/10.18168/bgi.23
Carlson R, Raskin G (1984) Density of the ocean crust. Nature 311(5986):555–558
Chen X, Liu Z, Zhang Z, Yang H, Hou F, Wang Z (2013) Deducing the East China Sea shelf basin by jointing gravity and seismic data. Progr Geophys (in Chinese) 28(03):1596–1601
Chen M, Fang J, He H (2019) Moho depths of the South China Sea and adjacent regions: results from gravity anomaly data. J Geodesy Geodyn Chin 39(04):356–360. https://doi.org/10.14075/j.jgg.2019.04.005
Cheng Y, Wu Z, Xu B, Dai Y, Chu Y, Zhang J, Chen M, Ma S, Sun W, Xu L (2023) The Mesozoic tectonic evolution of the East China Sea Basin: new insights from 3D seismic reflection data. Tectonophysics 848:229717. https://doi.org/10.1016/j.tecto.2023.229717
Commer M (2011) Three-dimensional gravity modelling and focusing inversion using rectangular meshes. Geophys Prospect. https://doi.org/10.1111/j.1365-2478.2011.00969.x
Corchete V (2022) Crust and upper mantle structure beneath the Yellow Sea, the East China Sea, the Japan Sea, and the Philippine Sea. Int Geol Rev 65:259 4. https://doi.org/10.1080/00206814.2022.2150900
Cribb J (1976) Application of the generalized linear inverse to the inversion of static potential data. Geophysics 41(6):1365–1369. https://doi.org/10.1190/1.1440686
Cui Y, Guo L (2019) A Wavenumber-domain iterative approach for rapid 3-D imaging of gravity anomalies and gradients. IEEE Access 7:34179–34188. https://doi.org/10.1109/access.2019.2904717
Dai M (2004) Inversion research for gravity and synthetical interpretation of two profiles in the area of East China Sea and its adjacency. Progr Geophys (in Chinese) 19(02):331–340
Ding H (2004) The characteristics of gravity and magnetic field in the East China Sea and the pre-cenozoic geological interpretation and research. Ph.D., Tongji University
Fang J (2002) Gravity feature and tectonic interpretation in China Sea and its adjacent regions. Progr Geophys (in Chin) 17(01):42–49
Fedi M (2007) DEXP: a fast method to determine the depth and the structural index of potential fields sources. Geophysics 72(1):I1–I11. https://doi.org/10.1190/1.2399452
Fei J, Fei L, Jin-Yao G, Qiao Z, Wei-Feng H (2018) 3-D density structure of the Ross Sea basins, West Antarctica from constrained gravity inversion and their tectonic implications. Geophys J Int 2:2. https://doi.org/10.1093/gji/ggy343
Gao D, Hou Z, Tang J (2000) Multiscale analysis of gravity anomalies on East China Sea and adjacent regions. Chin J Geophys 43(06):842–849. https://doi.org/10.1002/cjg2.105
Gao J, Zhang T, Fang Y, Yang C, Wang J, Tan Y, Mei S (2008a) Faulting, magmatism and crustal oceanization of the Okinawa Trough. Acta Oceanol Sin (in Chin) 30(05):62–70
Gao J, Wang J, Yang C, Zhang T, Tan Y (2008b) Discussion on back-arc rifting tectonics and its geodynamic regime of the Okinawa Trough. Progr Geophys (in Chin) 90(04):1001–1012
He H, Fang J, Chen M, Cui R (2019) Moho depth of the East China Sea inversed using gravity data. Geomat Informat Sci Wuhan Univ (in Chin) 44(05):682–689. https://doi.org/10.13203/j.whugis20170330
He H (2022) Research and Application of Forward and Inversion Method of Gravity Anomaly in the Wavenumber Domain. Ph.D., University of Chinese Academy of Sciences, http://dpaper.las.ac.cn/Dpaper/detail/detaINew?paperID=20210894
He H, Fang J, Guo D, Cui R, Xue Z (2024) 3D density imaging using gravity and gravity gradient in the wavenumber domain and its application in the Decorah. Sci Rep 14(134). https://doi.org/10.1038/s41598-023-49711-z
Johnson HP, Pruis MJ, Van Patten D, Tivey MA (2000) Density and porosity of the upper oceanic crust from seafloor gravity measurements. Geophys Res Lett 27(7):1053–1056. https://doi.org/10.1029/1999gl011130

Kobrunov AI (2015) The method of functional representations in the solution of inverse problems of gravimetry. Izv Phys Solid Earth 51(4):459–468. https://doi.org/10.1134/s1069351315030076
Kobrunov AI, Varfolomeev VA (1981) One approach of density equivalent representation and using it for gravity field interpretation. Earth Phys USSR Acad Sci 550(831):25–44
Laske G, Masters G, Ma Z, Pasyanos M (2013) Pasyanos M (2013) Update on CRUST1.0—A 1-degree global model of Earth's crust. Geophys Res 15(15):2658
Li J, He X, Huang J (2022) Adaptive weight density inversion method for gravity anomaly and mesozoic division of Diaobei Sag in East China Sea. J Jilin Univ (earth Sci Edn) 52(01):229–237. https://doi.org/10.13278/j.cnki.jjuese.20210018
Liang W, Li J, Xu X, Zhang S, Zhao Y (2020) A high-resolution Earth's gravity field model SGG-UGM-2 from GOCE, GRACE, satellite altimetry, and EGM2008. Engineering 6(8):860–878. https://doi.org/10.1016/j.eng.2020.05.008
Lin J-Y, Sibuet J-C, Hsu S-K (2005) Distribution of the East China Sea continental shelf basins and depths of magnetic sources. Earth Planets Space 57(11):1063–1072. https://doi.org/10.1186/BF03351885
Liu Z, Dai L, Li S, Li Z-H, Ding X, Bukhari SWH, Somerville I (2022) Earth's surface responses during geodynamic evolution: numerical insight from the southern East China Sea Continental Shelf Basin, West Pacific, Gondwana. Research 102:167–179. https://doi.org/10.1016/j.gr.2020.12.011
Minami H, Okada C, Saito K, Ohara Y (2022) Evidence of an active rift zone in the northern Okinawa Trough. Mar Geol. https://doi.org/10.1016/j.margeo.2021.106666
Nishizawa A, Kaneda K, Oikawa M, Horiuchi D, Fujioka Y, Okada C (2019) Seismic structure of rifting in the Okinawa Trough, an active backarc basin of the Ryukyu (Nansei-Shoto) island arc–trench system. Earth Planets Space 71(1):1–26. https://doi.org/10.1186/s40623-019-0998-6
Petrishchevsky AM (2022) The crust and upper mantle of the East China Sea (seismic tomography and gravity models). Russ J Pac Geol 16(5):465–476. https://doi.org/10.1134/s1819714022050062
Priezzhev I, Scollard A, Lu Z (2014) Regional production prediction technology based on gravity and magnetic data from the Eagle Ford formation, Texas, USA. Paper presented at the SEG Technical Program Expanded Abstracts 2014
Radhakrishna M, Subrahmanyam C, Damodharan T (2010) Thin oceanic crust below Bay of Bengal inferred from 3-D gravity interpretation. Tectonophysics 493(1–2):93–105. https://doi.org/10.1016/j.tecto.2010.07.004
Shang L (2014) Tectonics and Evolution of the Okinawa Trough. Ph.D., Ocean University of China
Shang L-N, Zhang X-H, Jia Y-G, Han B, Yang C-S, Geng W, Pang Y-M (2017) Late Cenozoic evolution of the East China continental margin: insights from seismic, gravity, and magnetic analyses. Tectonophysics 698:1–15. https://doi.org/10.1016/j.tecto.2017.01.003
Sibuet J-C, Zhao M, Wu J, Lee C-S (2021) Geodynamic and plate kinematic context of South China Sea subduction during Okinawa trough opening and Taiwan orogeny. Tectonophysics 817:229050. https://doi.org/10.1016/j.tecto.2021.229050
Suo Y, Li S, Cao X, Wang X, Somerville I, Wang G, Wang P, Liu B (2020) Mesozoic-Cenozoic basin inversion and geodynamics in East China: a review. Earth Sci Rev 210:103357. https://doi.org/10.1016/j.earscirev.2020.103357
Tozer B, Sandwell DT, Smith WH, Olson C, Beale JR, Wessel P (2019) Global bathymetry and topography at 15 arc sec: SRTM15+. Earth Space Sci 6(10):1847–1864. https://doi.org/10.1029/2019EA000658
Wang M, Jiang X, Lei B, Huang L, Pan J (2023) Tectonic evolution and its control on oil–gas accumulation in southern East China Sea since the Jurassic. Front Earth Sci 10:1015832. https://doi.org/10.3389/feart.2022.1015832
Xu G (2020) Features of gravity and magnetic field and theirtectonic implications of the Okinawa Trough. Master, China University of Geosciences (Beijing)
Yang J, Xu S, Yu H, Li H (2008) Application of apparent density inversion method in the East China Sea and its adjacent area. Chin J Geophys 51(6):1210–1219. https://doi.org/10.1002/cjg2.1318
Yang C, Han B, Yang C, Yang Y, Sun J, Yu F, Li S (2018) Mesozoic basin evolution of the East China Sea Shelf and tectonic system transition in Southeast China. Geol J 55(1):239–252. https://doi.org/10.1002/gj.3409
Yang C, Yang C, Yang Y, Sun J, Wang J, Xiao G, Wang J, Yuan Y (2022) Deep stratigraphic framework and hydrocarbon resource potential in the Southern East China Sea Shelf Basin. Mar Geol Quater Geol 42(05):158–171. https://doi.org/10.16562/j.cnki.0256-1492.2022060602
Yu H, Xu C, Chen H, Chai Y, Qin P, Wang G, Zhang H, Xu M, Xing C, Wang H (2023) Multilayer densities of the crust and upper mantle in the South China Sea using gravity multiscale analysis. Remote Sens 15(13):3274. https://doi.org/10.3390/rs15133274
Zhang G, Zhang J (2015) A discussion on the tectonic inversion and its genetic mechanism in the East China Sea Shelf Basin. Earth Sci Front 22(01):260–270. https://doi.org/10.13745/j.esf.2015.01.022
Zhang Y, Hu S, Liu J, Jiang Y, Chen Z, Qin J, Diao H, Wang C (2022) Geochemical characteristics and genesis of oil and gas in the Lishuixi Sag, East China Sea Shelf Basin. Geoscience 36(05):1382–1390. https://doi.org/10.19657/j.geoscience.1000-8527.2022.052
Zhu X, Wang L, Zhou X (2022) Structural features of the Jiangshao Fault Zone inferred from aeromagnetic data for South China and the East China Sea. Tectonophysics. https://doi.org/10.1016/j.tecto.2022.229252

Publisher's Note